

Application of Reliability-Based Topology Optimization for Microelectromechanical Systems

Chwail Kim*

University of Iowa, Iowa City, Iowa 52242-1527

and

Semyung Wang,[†] Ilhan Hwang,[‡] and Jonghyun Lee[§]

Gwangju Institute of Science and Technology, Gwangju 500-712, Republic of Korea

DOI: 10.2514/1.28508

In reliability-based design optimization, the constraints consider the probability of the satisfaction/failure of critical events. Lately, reliability-based design optimization has been applied to topology optimization, resulting in the development of reliability-based topology optimization. And though reliability-based topology optimization can be a useful and meaningful method, it requires excessive computational resources. Therefore, this research proposes a parallel-computed reliability-based topology optimization using the response surface method. This paper demonstrates that the proposed method greatly reduces the computation requirement of reliability-based topology optimization. The proposed methodology is then applied to design microelectromechanical systems. Specifically, in microelectromechanical systems, reliability-based topology optimization can be highly effective because of randomness generated during the etching process and scaling effect. The proposed method successfully designs new devices and verifies the designs via experiment.

Nomenclature

E_0	=	Young's modulus
G	=	limit state function (performance function) ($G > 0$)
g	=	constraint function ($g < 0$)
k_x	=	translational stiffness
k_θ	=	rotational stiffness
L_g	=	sum of the squares error of sensitivity
L_{new}	=	new least-squares function
L_y	=	sum of the squares error of function
P_f	=	probability of failure
P_{ft}	=	target probability of failure
P_s	=	system probability for success
P_{ts}	=	target probability for success
sw_g	=	weighting factor for the gradient
t	=	thickness
X	=	random variable (uncertain variable)
\mathbf{x}	=	approximation position vector
x	=	deterministic design variable or mean value of random variable
β_s	=	system reliability index for success
β_t	=	target reliability index for success
η_i	=	i th density function (design variable for topology)
μ_i	=	mean value of i th uncertain variable
σ_i	=	standard deviation of i th uncertain variable

I. Introduction

CLASSICAL optimization methodologies are based on deterministic methods, although the systems necessitate

probabilistic design methods due to randomness in loads, material properties, etc. Consequently, probabilistic design has been the source of extensive research. The objective of probabilistic design optimization is to obtain a safe design by considering the uncertain variables while also minimizing the cost function. One such probabilistic design method is reliability-based design optimization (RBDO). RBDO uses the same cost function as deterministic optimization, however, constraints consider the probability of the satisfaction/failure of critical response measures.

Most current research on RBDO uses the reliability index approaches (RIA). However, convergence problems are associated with the RIA even though a most probable point (MPP) exists. Additionally the RIA requires complicated sensitivity derivations and computations. Tu et al. [1,2] proposed the performance measure approach (PMA) as an inverse reliability analysis consistent with conventional RIA [3]. The convergence of PMA is better than RIA, and PMA does not require complicated sensitivity computation.

The concept of RBDO was applied to topology optimization, resulting in the so-called reliability-based topology optimization (RBTO) [4,5]. RBTO determines an optimal topology that satisfies a given probabilistic constraint given the uncertainties in multiphysics systems such as structural, electromagnetic, thermal, and coupled systems. As such, structural static [4], eigenvalue [4], magnetostatic energy [6], thermal temperature [7], and electric-thermal actuator problems [8] have all been solved using RBTO methodology. Maute and Frangopol [5] apply the RBTO methodology to design microelectromechanical systems (MEMS), and Jung and Cho [9] use it to design geometrically nonlinear structures. The RBTO designs are compared with the safety factor for a traditional design to examine the effectiveness of the RBTO method.

A major disadvantage of RBTO is the excessive computational time requirements. As such, this research proposes a parallel-computed RBTO using the response surface method (RSM) and then applies it to design MEMS. This paper sequentially explains the RBTO method, discusses the development of an advanced response surface method, provides details about the proposed method, designs MEMS with the method, and then presents conclusions.

II. Reliability-Based Topology Optimization

A. Concept of Reliability-Based Design Optimization

The goal of the engineering design is to control elements of a system such that the system performance satisfies various criteria for

Received 5 December 2006; revision received 30 July 2007; accepted for publication 4 August 2007. Copyright © 2007 by the American Institute of Aeronautics and Astronautics, Inc. All rights reserved. Copies of this paper may be made for personal or internal use, on condition that the copier pay the \$10.00 per-copy fee to the Copyright Clearance Center, Inc., 222 Rosewood Drive, Danvers, MA 01923; include the code 0001-1452/07 \$10.00 in correspondence with the CCC.

*Post Doctor, Center for Computer Aided Design, College of Engineering, AIAA Member.

[†]Professor, Department of Mechatronics, 1 Oryong-dong, Buk-gu; smwang@gist.ac.kr. Senior Member AIAA (Corresponding Author).

[‡]Ph.D Candidate, Department of Mechatronics, 1 Oryong-dong, Buk-gu.

[§]Professor, Department of Mechatronics, 1 Oryong-dong, Buk-gu.

safety, serviceability, and durability under numerous conditions. For example, a structure should be designed so that its strength or resistance will withstand the application of the applied loads. In reality, there are numerous sources of uncertainty when determining system parameters. For example, the load may be random. The goal of RBDO is to incorporate this uncertainty into the design.

RBDO uses the same cost function $f(x)$ and design variable x as in deterministic optimization, but it replaces the deterministic constraints $G(x) \geq 0$ with probabilistic constraints $P[G(X) < 0] \leq P_{ft}$.

The general RBDO problem reads

$$\begin{aligned} \min_x f(x) \quad & \text{subject to} \quad P_f(X) = P[G(X) < 0] \leq P_{ft} \\ & x_i^L \leq x_i \leq x_i^U \quad i = 1, \dots, n \end{aligned} \quad (1)$$

where P_{ft} is the target probability of failure of the constraint $G(X) \geq 0$, and x_i^L and x_i^U are the lower and upper limits of design variable x_i , respectively. The probabilistic constraint $P_f(X)$ is defined such that if the limit state function value $G(x)$ is smaller than 0, the system fails. The probability of failure in Eq. (1) is defined as

$$\begin{aligned} P_f(X) &= F_G(0) \\ &= \int \dots \int_{G < 0} f_X(X_1, X_2, \dots, X_n) dX_1 dX_2 \dots dX_n \leq P_{ft} \end{aligned} \quad (2)$$

where $F_G(0)$ is the probability that the limit stage function is smaller than 0 ($G < 0$), and f_X is the probability density function.

Additionally, the failure probability limit P_{ft} can be approximated by the target reliability index β_t as

$$\beta_t = -\phi^{-1}(P_{ft}) \quad (3)$$

where $\phi(\cdot)$ is the standard normal cumulative distribution function. Hence, the probabilistic constraint in Eq. (2) can be rewritten as

$$F_G(0) \leq \phi(-\beta_t) \quad (4)$$

Through inverse transformations, the above equation can be expressed in two ways [1,2] such that

$$\beta_s = -\phi^{-1}[F_G(0)] \geq \beta_t \quad (5)$$

or

$$G^* = F_G^{-1}[\phi(-\beta_t)] \geq 0 \quad (6)$$

where β_s is traditionally called the system reliability index [3], and G^* is the probabilistic performance measure.

In conventional RBDO methodology, probabilistic constraints are evaluated using Eq. (5), commonly known as RIA. Recently, Eq. (6) has been used to prescribe probabilistic constraints, the basis of a method referred to as the performance measure approach [1,2].

Therefore, the different formulations of RBDO can be described as follows:

For RIA,

$$\begin{aligned} \min_x f(x) \quad & \text{subject to} \quad \beta_s(X) \geq \beta_t \\ & x_i^L \leq x_i \leq x_i^U \quad i = 1, \dots, n \end{aligned} \quad (7)$$

For PMA,

$$\begin{aligned} \min_x f(x) \quad & \text{subject to} \quad G^*(X) \geq 0 \\ & x_i^L \leq x_i \leq x_i^U \quad i = 1, \dots, n \end{aligned} \quad (8)$$

B. Formulations of Reliability-Based Topology Optimization

Because conventional topology optimization [10] uses deterministic constraints, the RBDO method is applied to topology optimization to consider probabilistic constraints. And therefore, RBTO [3] can be interpreted as an approach used for finding an

optimum topology under probabilistic constraints such that the topology becomes reliable for these uncertainties.

The general form of an RBTO problem is described in the following equation:

Find the design variable vector $\eta = (\eta_1, \eta_2, \dots, \eta_n)$ such that

$$\begin{aligned} \min / \max \quad & f(\eta_i) \\ \text{subject to} \quad & P_s(X) = P[G(\eta_i, X_j) \geq 0] \geq P_t \quad 0 \leq \eta_i \leq 1 \quad (9) \\ & i = 1, \dots, ndv \quad \text{and} \quad j = 1, \dots, \text{no. of uncertain variables} \end{aligned}$$

where X_j is the j th uncertain variable, P_s is the system probability of success, P_t is the target probability of success, G is the limit state function (performance function), and ndv is the number of design variables.

Here, the design variables are the density functions η_i , in each finite element, and the performance functions depend on the physics in each system.

Thus, using RIA and PMA, Eq. (9) can be formulated in the following ways:

For RIA,

$$\begin{aligned} \min / \max \quad & f(\eta_i) \\ \text{subject to} \quad & \beta_s(\eta_i, X_j) \geq \beta_t \\ & \text{when } G(X) = 0 \text{ for each evaluation} \\ & 0 \leq \eta_i \leq 1 \\ & i = 1, \dots, ndv \quad \text{and} \quad j = 1, \dots, \text{no. of uncertain variables} \end{aligned} \quad (10)$$

For PMA,

$$\begin{aligned} \min / \max \quad & f(\eta_i) \\ \text{subject to} \quad & G^*(\eta_i, X_j) \geq 0 \\ & \text{when } \beta_s = \beta_t \text{ for each evaluation} \\ & 0 \leq \eta_i \leq 1 \\ & i = 1, \dots, ndv \quad \text{and} \quad j = 1, \dots, \text{no. of uncertain variables} \end{aligned} \quad (11)$$

where β_s is the system reliability index for success and β_t is the target reliability index for success.

PMA has a number of advantages [1,2] compared to RIA: the convergence of the solution and overall computational efficiency. For these reasons, PMA is the primary approach used for RBDO and RBTO in this research.

To solve an RBTO problem, the performance (or limit state) function should first be defined, and a sensitivity analysis should be performed with respect to each uncertain variable [4].

For a static problem, the performance function can be defined by

$$G = -U + U_{\max} \geq 0 \quad (12)$$

where U is the displacement at a target point.

Note that the limit state in Eq. (12) implies that if the displacement U is larger than the limit value U_{\max} , the system fails.

III. Advanced Response Surface Method

The RSM [11] is a well-known meta-modeling technique. However, the approximation error inherent in this method has placed a number of restrictions on designers due to the fact that classical RSM uses the least-squares method (LSM) to find the best-fit approximation models from among all the given data. In previous research, the authors have suggested how to construct a response surface (RS) model more efficiently and accurately using the moving least-squares method (MLSM) with sensitivity information [12].

The MLSM can be explained as a weighted LSM that has various weights with respect to the position of approximation. And therefore, MLSM can represent local responses. For sampled data, only one global approximation curve can be obtained from LSM. On the other

hand, in MLSM, there exists one approximation function at each calculation point. Therefore, the coefficients of the RS model vary with the calculation location. This locally weighted approximation can be performed based on the consideration of effective data near the calculation location, and the data are weighted according to the distance from the calculation location.

If the sensitivity (gradient) of each sampling point can be calculated efficiently [13], then the sensitivity and function (response) data can be used to construct an RS model. Because the sensitivities have higher order information than the function values, accurate sensitivities can effectively increase the accuracy of RS. The main idea of a sensitivity-based RS is to minimize the function errors and sensitivity using MLSM. This concept is explained by the following equation:

$$\begin{aligned} &\text{Find a function s.t.} \\ &\text{minimize } L_{\text{new}}(\mathbf{x}) = (1 - sw_g)L_y(\mathbf{x}) + sw_gL_g(\mathbf{x}) \end{aligned} \quad (13)$$

where L_{new} is a new least-squares function, L_y is the sum of the squares error of the function, L_g is the sum of the squares error of sensitivity, \mathbf{x} is an approximation position vector, and sw_g is a weighting factor for the gradient [12].

IV. Parallel-Computed Reliability-Based Topology Optimization Using the Response Surface Method

A. Concept of the Proposed Method

Although RBDO and RBTO can be applied to many fields, they both require expensive computational time. Because recent engineering processes demand faster development and manufacturing of products, long computational time requirements can be a serious problem. Thus, in this research the method proposed for reducing the design time is parallel computed RBTO using RSM. The basis of this method is that parallel computing can reduce analysis time by using several analyzers, and the RSM approach can further reduce the time demand by approximating multiple responses.

Figure 1 illustrates the overall system. In the figure, RBTO is a bilevel optimization problem, as it has two loops of optimization. The outer loop is related to the determination of the optimal topology, and the inner loop is related to the analysis of the system reliability. The results from each of the parallel machines are gathered and used

to construct an RS model for the reliability analysis at each iteration of optimization. Therefore, no additional sampling or computation is required for the sensitivity of the reliability analysis because RS is used for the reliability analysis. (The computational time for RS can be ignored because RS is just a calculated mathematical function.)

RBTO adopts an adjoint variable method [4,13] for the design sensitivity for topology optimization and therefore only one additional adjoint analysis is required under the unit load for a linear static problem. Note that this adjoint analysis is automatically distributed to the parallel computers. Eventually, the proposed method does not require a large amount of computation for the sensitivity analysis and this is an advantage of the proposed method.

Though this process can save computational time, the reliability calculated using RS has approximation errors, and to compensate for these errors, this research adopts the previously introduced MLSM.

Whereas this process can save computational time, the reliability calculated using RS has approximation errors. Therefore, to compensate for these approximation errors, this research adopts the previously introduced MLSM.

In Fig. 1, conventional RBDO using RSM is illustrated using dotted lines, and RBDO proceeds using the initially constructed RS. However, in RBTO, RS is reconstructed at each iteration due to the change in topology at each iteration. In the figure, the inner loop represents a reliability analysis (precisely, an inverse reliability analysis because the research used PMA), which is a suboptimization loop.

DOT, commercial optimization software [14], is used for the outer loop optimization.

In this research, the proposed RBTO technology is applied to MEMS. Specifically, the consideration of uncertainties is important in MEMS due to the presence of inherent problematic characteristics found in the etching process and the scaling effect.

B. Parallel Computing System

The primary purpose of the parallel computing system is to construct an inexpensive system using PCs (personal computers), and to distribute jobs to the computers on the network. Therefore, PC-based TCP/IP socket programming is adopted, and C/C++ using Microsoft foundation class (MFC) in Visual C++ is used. The main tasks of the system are as follows: 1) socket programming—server/client, 2) multithread control, 3) analysis job management, and 4) data loss (packet loss) checking.

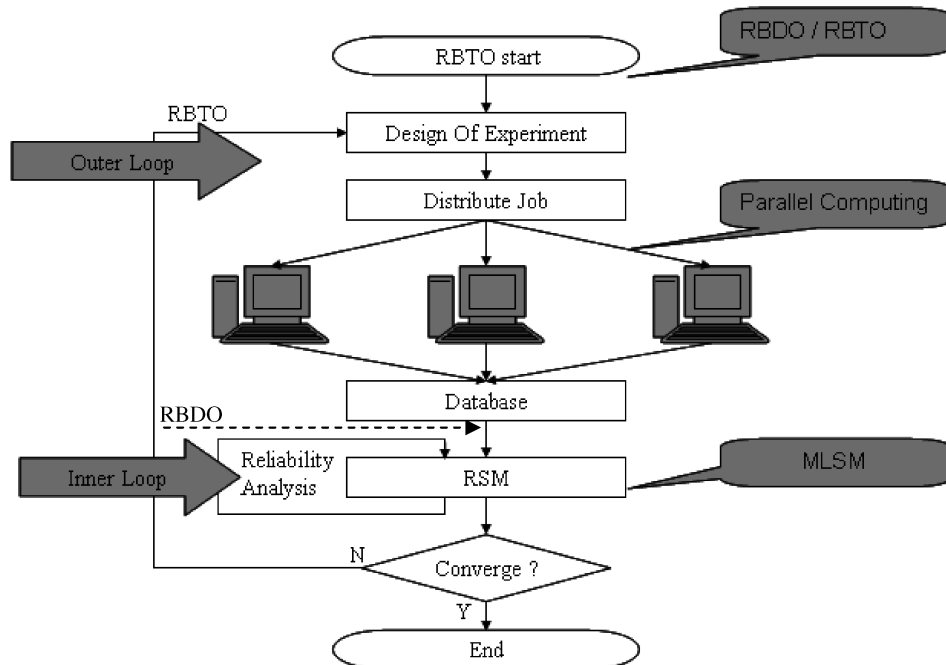


Fig. 1 Flowchart of parallel-computed RBTO using RSM.

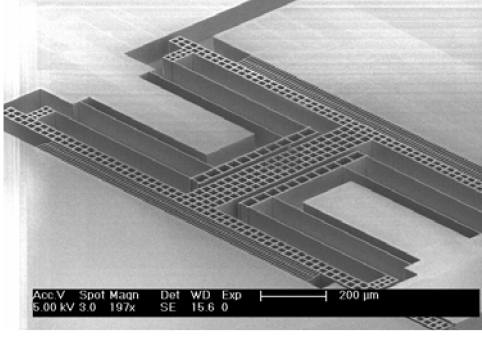


Fig. 2 Scanning electron microscope (SEM) image of a double-folded-spring (DFS) structure.

This research used a classical data communication method between server and client in the socket programming. A sever is an analysis server in a remote machine and the server program should be installed on each parallel machine.

In this research, the client can ask for file uploading, remote execution, and file downloading. If a main computer commands a client to do remote works, each multithreaded client asks each server for input file uploading, remote analysis, and result file downloading.

V. Application Examples

A. System and the Overall Design Process

In MEMS, many types of actuators are employed to achieve the desired motions of a device, which include comb actuators and parallel actuators, among others. When an electrical input is applied to the actuators, flexible parts of the system connected to the actuators experience deflections and store the potential energy in their structures. Subsequently, when the electrical inputs are turned off, the deflected flexible parts return to their initial positions and release their stored potential energy.

As representative designs of flexible structures in MEMS, simple-beam-spring or double-folded-spring (DFS) structures are widely employed [15]. In a simple-beam-spring structure, the spring stiffness increases with the amount of beam deflection and requires a greater force than the theoretical value for the displacement of the shuttle mass connected to the springs. However, in the DFS structure shown in Fig. 2, a couple of simple beams are serially connected such that each simple beam shares the total deflection. As a result, a lesser amount of spring stiffness can be expected for the same displacement of shuttle mass. Therefore, for structures experiencing large displacements, DFS structures are superior in terms of their linearity of control and motion.

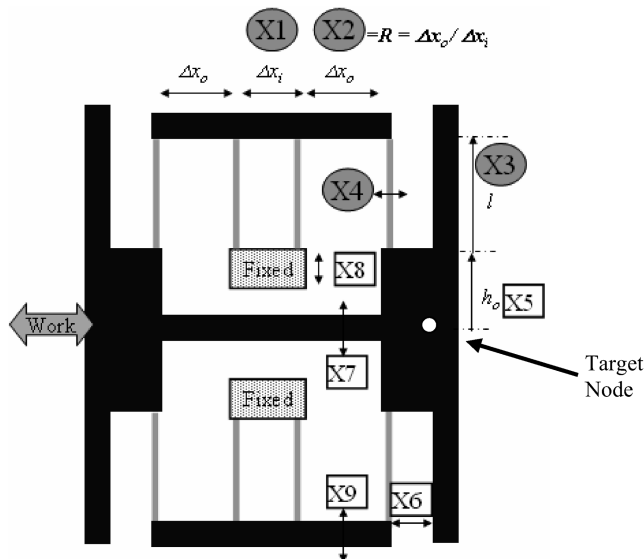


Fig. 3 Design variables for RBDO.

Table 1 Design domain for RBDO

Design variable, μm	Lower limit	Upper limit
X1 (inner length)	100	250
X2 (outer length ratio)	0.5	2.0
X3 (spring length)	100	150
X4 (spring thickness)	2	4

Nevertheless, even though DFS structures are effective in achieving high linearity, rotational stability has not yet been thoroughly investigated. Rotational instability may be evident in situations where the shuttle mass is displaced by comb or parallel actuators, and as a result the spring structures do not provide sufficient rotationwise stability; the two electrodes of the actuators might contact each other and cause a short in the electrical system. Hence, DFS structures should have maximum spring stiffness in the rotation direction, with the required spring stiffness in the actuation direction parallel to the shuttle mass. For spring stiffness in the actuation direction, the main design parameters include the length, width, and height of the spring structure. However, for the spring stiffness in the rotation direction, the position of each spring beam can be another primary design parameter.

Thus, if these design parameters can be optimized so that the spring structures have maximum spring stiffness in the rotation direction for the required spring stiffness in the actuation direction, DFS structures can attain optimum stability.

To determine the optimum stability, RBDO is first performed based on the sizing point of view of the system, and then the proposed RBTO is performed to determine a new type of structure. Next, the results of RBTO are transformed to a reanalysis model, and finally, real devices are fabricated and tested based on the designed model.

B. RBDO of a Double-Folded-Spring System

The structure of the system is shown in Fig. 3. As illustrated, there are nine variables, X1–X9, that determine the shape of the system, with four variables, X1–X4, selected from a screening test. The selected variables are dominant to the rotational stiffness k_θ and translational stiffness k_x . The variables are defined in Fig. 3, and their lower and upper design limits are given in Table 1.

To calculate stiffnesses, k_θ and k_x , two different force sets, are applied to the system, as shown in Fig. 4. Force set 1 is applied to calculate k_x , and Fig. 4a shows that a single force is applied to the center of the shuttle. The X-directional displacement of the target node (the circled node in Figs. 3 and 4) is inversely proportional to k_x . Force set 2 is applied to calculate k_θ , and Fig. 4b shows that the two applied forces impose a torsion effect. The Y-directional displacement of the target node is inversely proportional to k_θ .

Optimization problems are then set up to maximize k_θ ($\mu\text{N} \cdot \mu\text{m}$), which is equal to minimize the Y-directional displacement at the target node. Here, k_x ($\mu\text{N}/\mu\text{m}$) is considered as a constraint to satisfy the given actuation stiffness. The problem definition is given in Eq. (14). ANSYS, commercial finite element software, is used as an

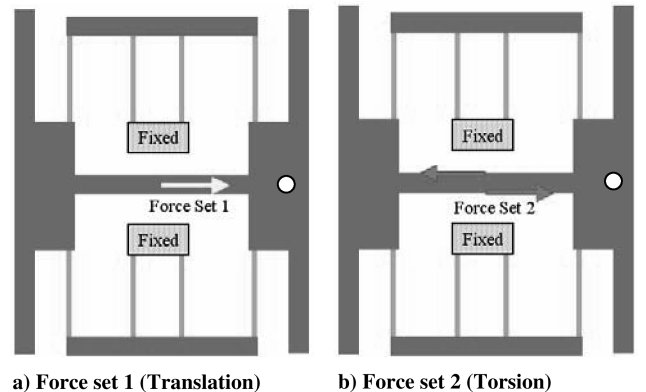


Fig. 4 Cases of applied force.

Table 2 Comparison of RS accuracy

CRSM	$k_\theta, \mu\text{N} \cdot \mu\text{m}$	$k_x, \mu\text{N}/\mu\text{m}$	$g1 < 0$	$g2 < 0$
RSM prediction	1.268E + 100	2.316E + 002	−14.898	−0.002999
True value	1.290E + 010	2.453E + 002	−29.374	12.312
Error, %	−1.715	−5.594	—	(Violated)
MLSM	k_θ	k_x	$g1 < 0$	$g2 < 0$
RSM prediction	1.275E + 100	2.339E + 002	−19.489	−0.002999
True value	1.279E + 010	2.349E + 002	−19.758	1.102
Error, %	−0.2738	−0.3852	—	(Acceptable)

analyzer, and DOT, commercial optimization software, is used as an optimizer.

Specifically, MEMS devices require probabilistic design technology due to their inherent characteristics, fabrication errors can cause probabilistic uncertainties, and scaling effects make small dimensional uncertainties appear as large performance errors. In this example, RBDO using RSM is adopted to handle these uncertainties.

Deterministic and RBDO problems are defined as the following:

Deterministic optimization:

$$\begin{aligned} &\text{maximize } k_\theta, && \text{under force set 2} \\ &\text{subject to } 200 < k_x < 250, && \text{under force set 1} \end{aligned} \quad (14)$$

RBDO (PMA) case 1:

$$\begin{aligned} &\text{maximize } k_\theta, && \text{under force set 2} \\ &\text{subject to } 200 < k_x < 250, && \text{under force set 1} \\ &\text{when } \beta_i = 1.5, \quad \sigma_i = 0.01 \times \mu_i, \quad i = 1, \dots, ndv \end{aligned} \quad (15)$$

RBDO (PMA) case 2:

$$\begin{aligned} &\text{maximize } k_\theta, && \text{under force set 2} \\ &\text{subject to } 200 < k_x < 250, && \text{under force set 1} \\ &\text{when } \beta_i = 1.5, \quad \sigma_i = 0.02 \times \mu_i, \quad i = 1, \dots, ndv \end{aligned} \quad (16)$$

For RBDO problems, all four design variables are uncertain variables that have 1–2% standard deviations under normal distributions. The target reliability index is set to 1.5, meaning that the probability of success should be greater than 93.3%.

For RS construction, 30 points are sampled by the Latin hypercube design for the four design variables. Three defined optimization problems are solved using RSM, and RS accuracies are compared. Table 2 compares the difference between conventional RSM (CRSM) and MLSM for the RBDO (PMA) case 1 problem.

As can be seen in Table 2, the error of the CRSM at optimum is about 5.594% and can be considered a small error. However, the constraint functions ($g1$, $g2$) at MPP, which should be less than zero, have large errors. Specifically, the active constraint $g2$ is significantly violated (12.312%), thus, the optimum obtained using CRSM cannot be considered acceptable.

Conversely, the response errors using MLSM are less than 0.4%, and the active constraint $g2$ at MPP has a small error. Therefore, the optimum obtained using MLSM is deemed a reasonable solution.

For this problem, RS methodology is quite necessary because the total number of RS function calls is 3229; there are two probabilistic constraints requiring separate reliability analyses, resulting in a large number of RS function calls. Because an efficient sensitivity analysis is difficult for this problem, the finite difference method (FDM) is applied [13]. The constructed RS models can be reused for different optimization problems, and, as such, RSM is very efficient for this case. Because of the demand for accuracy, conventional RSM using LSM cannot be used, although MLSM gives an accurate solution.

The initial, deterministic, and probabilistic optimization results are given in Fig. 5 and Table 3. Table 3 shows that $X1$ converged to its upper limit because $X1$ significantly increases the k_θ . The deterministic optimum satisfies the constraint value (k_x is 250.9) at the mean values of X . However, RBDO optimums show safer constraint values (k_x are 234.9 and 223.3) at the mean values because these optimal designs satisfy the constraints at the MPP points.

C. Parallel-Computed RBTO of the Double-Folded-Spring System

The conventional DFS system given in the previous example was optimized using RBDO and RS methodologies. Now, with the design initially obtained by RBDO, RBTO methodology is applied to find a new type of device that has increased performance.

In this system, the spring is the most important part with respect to the overall system performance (k_θ and k_x). Therefore, the spring is selected as a design domain of the topology optimization, as shown in Fig. 6.

The basis model for topology optimization is obtained from the results of RBDO case 2 in the previous example. However, because the RBDO result is too large with respect to length x , an approximately half-sized model is created from the original RBDO model to fabricate more devices from one wafer. This reduced model is given in Fig. 7b, and the design domain from that reduced model is shown in Fig. 7c.

Three topology optimization problems are solved: 1) deterministic topology optimization (DTO), 2) RBTO with $\beta_i = 1.0$, and 3) RBTO with $\beta_i = 1.5$. Here, the number of design variables is 3400. The system should be symmetric and, as such, the symmetric condition is internally imposed. The uncertain variables are Young's modulus E , thickness t , and loading F , and the uncertain variables have 5% standard deviation of the mean values with normal distributions.

In the following equations, UX (μm) is the x -directional displacement of the target node and is inversely proportional to k_x . This property is associated with the actuation of the device. In

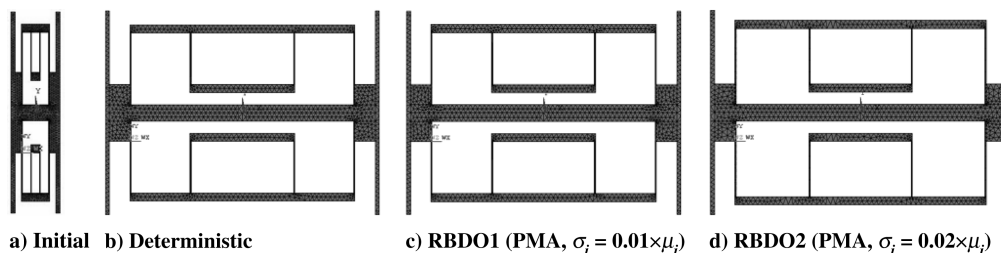


Fig. 5 RBDO results (geometry).

Table 3 RBDO results [design variables (DV) and performances]

DV/performances	Initial	Deterministic	RBDO 1 ($\sigma_i = 0.01 \times \mu_i$)	RBDO 2 ($\sigma_i = 0.02 \times \mu_i$)
X1 (inner length)	20	249.9	249.9	250.0
X2 (outer length ratio)	1	0.5770	0.5856	0.7206
X3 (spring length)	100	126.1	127.9	135.8
X4 (spring thickness)	2	2.707	2.686	2805
k_θ	1.162E + 08	1.304E + 10	1.279E + 10	1.260E + 10
k_x at X_{mean} value	202.9	250.9	234.9	223.3

addition, UY (μm) is the y -directional displacement of the target node and is inversely proportional to k_θ , associated with the stability of the device. The target value of the constraint is selected from the analysis result of the reduced model, as represented by Fig. 7b. Note that UY of the reduced model under force set 2 is $8.428\text{E}-06$ (μm).

Deterministic topology optimization:

$$\begin{aligned} \max \quad & UX && \text{(under force set 1: translation)} \\ \text{s.t.} \quad & UY < 8.0\text{E} - 6 && \text{(under force set 2: torsion)} \end{aligned} \quad (17)$$

RBTO using PMA:

$$\begin{aligned} \max \quad & UX && \text{(under force set 1: translation)} \\ \text{s.t.} \quad & UY < 8.0\text{E} - 6 && \text{(under force set 2: torsion)} \\ & \text{when } \beta = \beta_i \text{ (1.0 and 1.5)} \\ & \sigma_i = 0.05 \times \mu_i, \quad i = 1, 2, 3 \end{aligned} \quad (18)$$

In actuality, this problem requires a number of computations because the objective and constraints have different force sets, which need different analyses. Additionally, each response requires sensitivities for the reliability analysis and optimization. As time increases, the total number of computations can become very expensive requiring a significant amount of time, but the proposed method can be used to overcome this problem. Therefore, the proposed method, parallel-computed RBTO using RSM, is applied.

To construct RS, the D-optimal design of experiment (DOE) [11] determines five samplings for three uncertain variables. These five

Table 4 Time and efficiency of parallel computing

No. of computers	1	2	3
Elapsed time, s	572	307	221
Machine efficiency	1.00	0.932	0.863

Table 5 Error of RS for RBTO

	RSM (MLSM)	True	Error, %
Obj(UX)	—	$3.601\text{E} - 02$	—
Con(UY), X_{mean}	$7.316\text{E} - 06$	$7.323\text{E} - 06$	$-9.157\text{E} - 02$
Con(UY), MPP	$7.990\text{E} - 06$	$7.983\text{E} - 06$	$9.355\text{E} - 02$

analyses are obtained from three parallel computers using parallel computing at each iteration.

Table 4 shows the time and efficiency of the parallel computing system for one iteration of optimization. The machine efficiency in the table is computed as

$$\text{efficiency} = \text{time for one computer case} / (\text{no. of computers} \times \text{elapsed time}) \quad (19)$$

As can be seen in the table, if the number of computers increases, the machine efficiency decreases; this is a common characteristic of parallel computing. However, the parallel computing system is computationally useful because the elapsed time is reduced from 572 to 221 s. As such, this research adopts a parallel computing system for the purpose of reducing computational time.

The approximation error of RS is a problem in the proposed method; if RS has large errors, RBTO cannot be successfully completed. Here, MLSM is applied and the approximation error of RS is examined, as shown in Table 5. The table shows the error of RS at the mean point X and at MPP. Note that both errors are less than 0.1%, implying that the constructed RS is very accurate. Therefore, the RBTO result can be successfully obtained using MLSM.

Table 6 and Fig. 8 summarize the obtained results. In the table and Fig. 8, RBDO' refers to the reduced RBDO model shown in Fig. 7b. Figure 8, presenting the DTO results, shows a slightly declined inner spring. In addition, RBTO $\beta_i = 1.0$ shows an additional spring between the two vertical springs, and RBTO $\beta_i = 1.5$ shows the two separated springs of the inner spring.

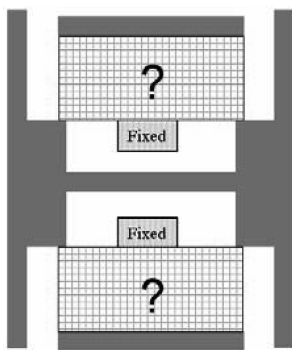
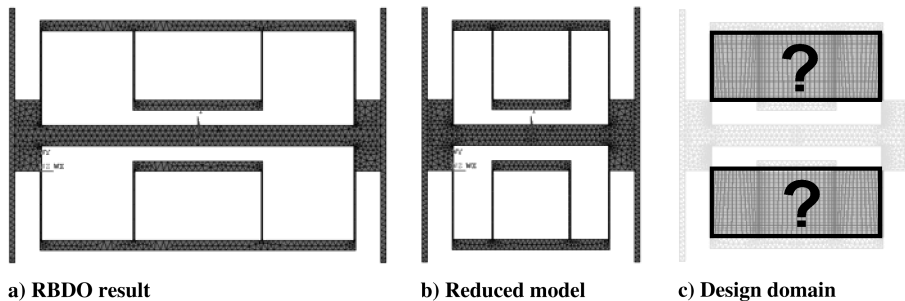
**Fig. 6 Design domain for topology optimization.****Fig. 7 Basis model and design domain for topology optimization.**

Table 6 Comparison of topology designs (values)

	Initial	RBDO'	DTO	RBTO $\beta_t = 1.0$	RBTO $\beta_t = 1.5$
UX	0.2463	0.02209	0.1473	0.03601	0.02270
UY	$0.8600E - 04$	$8.428E - 06$	$7.974E - 06$	$7.323E - 06$	$6.951E - 06$
k_x	202.9	226.3	33.95	138.85	220.3
k_θ	$1.162E + 08$	$4.878E + 09$	$5.157E + 09$	$5.615E + 09$	$5.910E + 09$

Because topology optimization results commonly contain a gray area, it is not appropriate to commence fabrication at this time. To remedy this situation, a reanalysis model is constructed to fabricate a real model from the results of RBTO $\beta_t = 1.5$. The reanalysis model and analysis results are given in Fig. 9.

The analysis results of Fig. 9b are $k_x = 218.1$ and $k_\theta = 5.870E + 09$, and these are very close to the results of RBTO. Therefore, it was determined that the reanalysis model is suitable for fabrication, and so several models were subsequently fabricated and tested.

D. Fabrication and Experiments of the Designed Model

To evaluate the rotational stiffness of the devices, the designed DFS systems were fabricated using silicon-on-insulator wafers with an $80\text{ }\mu\text{m}$ silicon structure layer, and a $3\text{ }\mu\text{m}$ silicon dioxide sacrificial layer on a $500\text{ }\mu\text{m}$ silicon substrate. Five types of DFS systems (initial, deterministic, RBDO 2, RBDO', and the RBTO-reanalysis model) were fabricated, and Fig. 10 presents three representative models from among the five types. One photo mask was used to make the etch mask on the silicon structure layer, and the silicon structure layer was then etched using a deep reactive ion etching (DRIE) process. The device was dry released using a gas phase etching machine [16].

A pair of parallel plate actuators was connected to either end of the shuttle mass to rotate the DFS system counterclockwise, by generating an electrostatic force with the same magnitude in the opposite direction. An optical fiber was inserted into the trench perpendicular to the mirror. Then, from the wavelength shift of the interference patterns between the sidewall of the mirror and the end of the optical fiber before and after actuation, the lateral displacement could be measured to evaluate the rotation angle [17].

Figure 11a shows the experimental results of the lateral displacement with respect to the driving voltage for the parallel plate actuators. It was determined that the lateral displacement increased with the driving voltage by amounts corresponding to the different rotational stiffness of each model. In addition, Fig. 11b shows the rotational stiffness evaluated from the lateral displacement and the magnitude of the electrostatic force. Each model showed little variation in rotational stiffness with respect to the driving voltage, and therefore the fabricated devices were deemed stable. Note that the values of the rotational stiffness from the experiments were not exactly the same as with a finite element analysis (FEA), though the ratios of the rotational stiffness between the models were almost the same for FEA and the experiments. In this study, the errors between FEA and the experiments could potentially be attributed to several

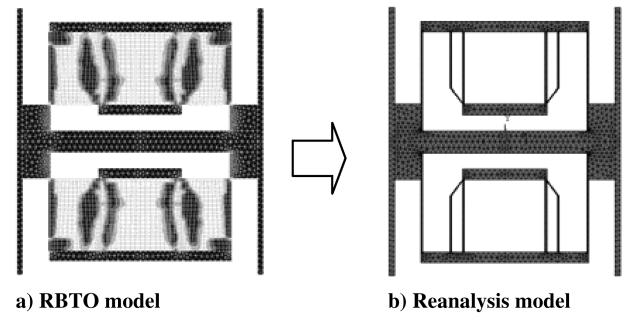
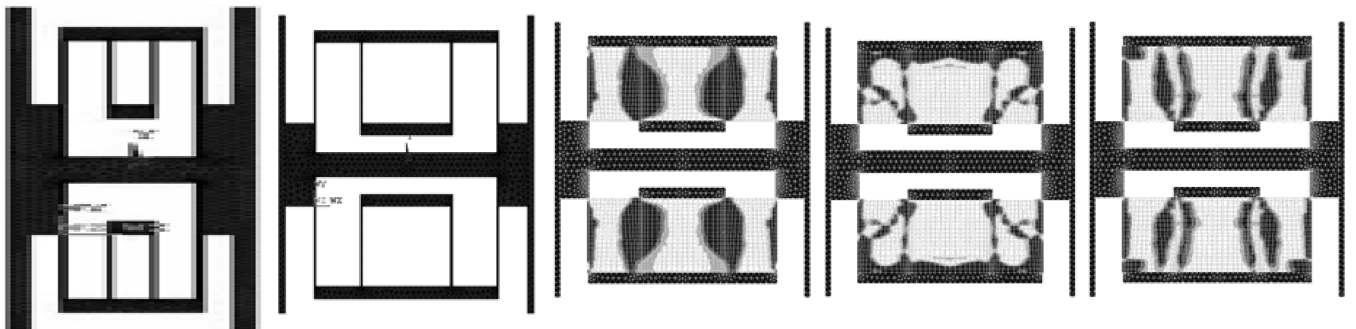
factors: different conditions between FEA and the experiments, assumption of rigid body parts for FEA, modeling errors, and fabrication errors [18]. Nevertheless, the important fact here is that the proposed method successfully designed new types of devices, and their performance was verified by subsequent fabrication and experimental analysis.

VI. Conclusions

In this research, the reliability-based design optimization (RBDO) concept was applied to topology optimization, resulting in the development of reliability-based topology optimization (RBTO). RBTO was then used to determine an optimal topology that satisfies the given probability of a case that considers uncertainties.

RBTO can be a useful and meaningful method, but it requires expensive computational time. Therefore, this research proposes parallel-computed RBTO using the response surface method due to the fact that parallel computing can reduce the processing time in the optimal design. RBTO is a bilevel optimization problem because it has two loops of optimization; the outer loop is related to determining the optimal topology, whereas the inner loop focuses on the analysis of the system reliability. Here, the inner loop proceeds based on RS approximation using the parallel-computed results. The separated analysis results from the parallel machines are then gathered and used to construct RS for the reliability analysis at each iteration. This process can save time, but the reliability from RS has approximation errors. And to compensate for these errors, this research adopts the developed RSM technology using the moving least-squares method.

The proposed RBTO methodology was subsequently applied to MEMS and structural systems. Specifically, in MEMS, RBTO was found to be highly effective in overcoming problematic system characteristics inherent in the etching process and the scaling effect.

**Fig. 9** Reanalysis model based on the RBTO results.**Fig. 8** Summary of topology designs.

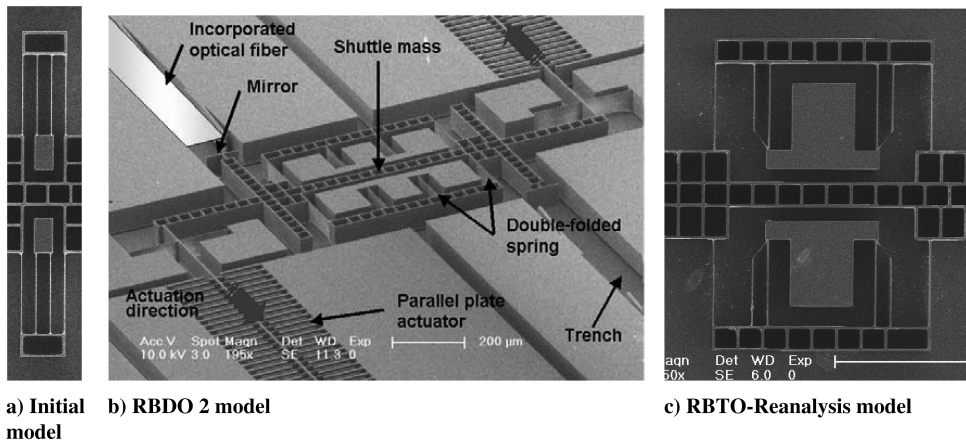


Fig. 10 SEM image of the fabricated double-folded springs with the aligned optical fiber for displacement measurement.

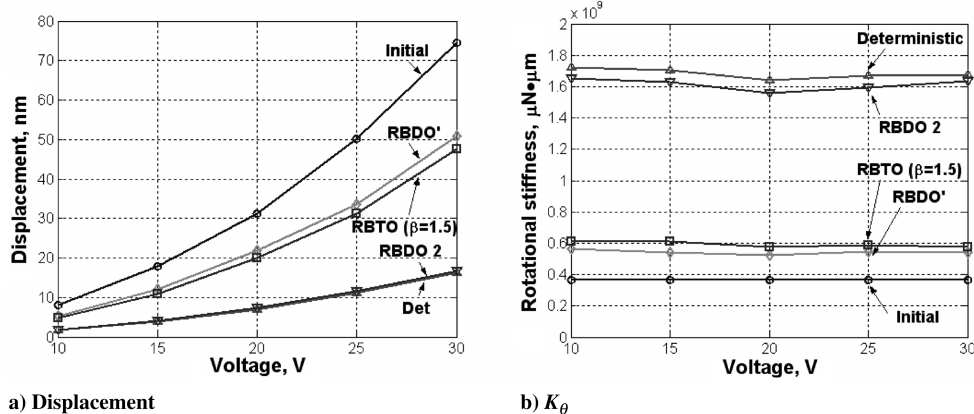


Fig. 11 Experimental results of the double-folded springs with respect to the driving voltage.

Analysis of the results confirmed that the proposed method determined new types of double-folded-spring systems while reducing computational time. Furthermore, from the RBTO results, a reanalysis model was constructed, and five types of models were subsequently fabricated and tested. The experimental results were shown to have the same trends as compared to the FEA results, even though the stiffness values of FEA were slightly different from experiment; thus, new types of devices were successfully designed using the proposed method.

Acknowledgments

This research was supported by the Center of Innovative Design Optimization Technology (iDOT), of the Korea Science and Engineering Foundation.

References

- [1] Tu, J., and Choi, K. K., "A New Study on Reliability-Based Design Optimization," *ASME Journal of Mechanical Design*, Vol. 121, No. 4, 1999, pp. 557–564.
- [2] Tu, J., Choi, K. K., and Park, Y. H., "Design Potential Method for Robust System Parameter Design," *AIAA Journal*, Vol. 39, No. 4, 2001, pp. 667–677.
- [3] Haldar, A., and Mahadevan, S., *Probability, Reliability and Statistical Methods in Engineering Design*, Wiley, New York, 2000.
- [4] Kim, C., Wang, S., Bae, K., Moon, H., and Choi, K. K., "Reliability-Based Topology Optimization with Uncertainties," *Journal of Mechanical Science and Technology*, Vol. 20, No. 4, April 2006, pp. 494–504.
- [5] Maute, K., and Frangopol, D. M., "Reliability-Based Design of MEMS Mechanisms by Topology Optimization," *Computers and Structures*, Vol. 81, Nos. 8–11, 2003, pp. 813–824. doi:10.1016/S0045-7949(03)00008-7
- [6] Kang, J. N., Kim, C. I., and Wang, S. M., "Reliability-Based Topology Optimization for Electromagnetic Systems," *COMPEL—The International Journal for Computation and Mathematics in Electrical and Electronic Engineering; Multilingua*, Vol. 23, No. 3, 2004, pp. 715–723. doi:10.1108/03321640410540647
- [7] Moon, H. G., Kim, C. I., and Wang, S. M., "Reliability-Based Topology Optimization of Thermal Systems Considering Convection Heat Transfer," *AIAA Paper 2004-4410*, Aug. 2004.
- [8] Moon, H. G., Kim, C. I., and Wang, S. M., "Reliability-Based Topology Optimization of a Thermoelastic Actuator," *6th World Congress of Structural and Multidisciplinary Optimization (WCSMO6)* [CD-ROM] 2005.
- [9] Jung, H. S., and Cho, S. H., "Reliability-Based Topology Optimization of Geometrically Nonlinear Structures with Loading and Material Uncertainties," *Finite Elements in Analysis and Design*, Vol. 41, No. 3, 2004, pp. 311–331. doi:10.1016/j.finel.2004.06.002
- [10] Bendsoe, M., and Sigmund, O., *Topology Optimization—Theory, Methods and Applications*, Springer, New York, 2003.
- [11] Myers, R. H., and Montgomery, D. C., *Response Surface Methodology: Process and Product Optimization Using Designed Experiments*, Wiley, New York, 1995.
- [12] Kim, C., Wang, S., and Choi, K. K., "Efficient Response Surface Modeling by Using Moving Least-Squares Method and Sensitivity," *AIAA Journal*, Vol. 43, No. 11, 2005, pp. 2404–2411.
- [13] Haug, E. J., Choi, K. K., and Komkov, V., *Design Sensitivity Analysis of Structural Systems*, Academic Press, Orlando, FL, 1986.
- [14] DOT user's manual, VR&D.
- [15] Tang, W. C., Nguyen, T. H., and Howe, R. T., "Laterally Driven Polysilicon Resonant Microstructures," *Proceedings of IEEE MEMS Conference*, IEEE, Piscataway, NJ, 1989, pp. 53–59.

- [16] Lee, J. H., Jang, W. I., Lee, C. S., Lee, Y. I., Choi, C. A., Baek, J. T., and Yoo, H. J., "Characterization of Anhydrous HF Gas-Phase Etching with CH₃OH for Sacrificial Oxide Removal," *Sensors and Actuators A (Physical)*, Vol. 64, No. 1, 1998, pp. 27–32.
doi:10.1016/S0924-4247(98)80054-X
- [17] Hwang, I. H., Yoon, E. S., and Lee, J. H., "A Micromachined Reaction Force Actuator (RFA) for Nano Manipulator," *Journal of Microelectromechanical Systems*, Vol. 15, No. 3, 2006, pp. 492–497.
doi:10.1109/JMEMS.2006.872236
- [18] Chen, K. S., Ayon, A. A., Zhang, X., and Pearing, S. M., "Effect of Process Parameters on the Surface Morphology and Mechanical Performance of Silicon Structures After Deep Reactive Ion Etching," *Journal of Microelectromechanical Systems*, Vol. 11, No. 3, 2002, pp. 264–275.
doi:10.1109/JMEMS.2002.1007405

J. Samareh
Associate Editor